The stability of MEA in SPE water electrolysis for hydrogen production

Guoqiang Wei [a,b], Yuxin Wang [a,b], Chengde Huang [a], Qijun Gao [a,b], Zhitao Wang [a,b], Li Xu [a,*]

[a] School of Chemical Engineering and Technology, Tianjin University, No. 92 Weijin Road, Tianjin 300072, PR China
[b] State Key Laboratory of Chemical Engineering, Tianjin University, Tianjin 300072, PR China

ABSTRACT

Membrane electrode assemblies (MEAs) for water electrolysis were prepared by decal transferring an Ir black anode and a Pt black cathode on the two sides of a perfluorosulfonate solid polymer electrolyte (SPE) Nafion112 membrane. Performance stability of an MEA with 4 cm^2 effective electrode area was tested for 208 h in a single cell water electrolysis setup. The catalysts of both electrodes on the MEAs were characterized by means of XPS and XRD. Samples of feed water were analyzed by using conductivity meter, inductance coupling plasma optical emission spectroscopy (ICP-OES), ionic chromatography and total organic carbon (TOC) analyzer. Surface oxidation of the anodic Ir catalyst was evidenced, from the original metal Ir to 71.5% Ir$_2$O$_3$ and 28.5% IrO$_2$ after 208 h of electrolysis. While the metallic state of Pt on the cathode did not change during the same period of operation, the crystallite size of the Pt catalyst increased from 9.1 nm to 9.8 nm. Water analysis shows there is significant accumulation of impurities in the feed water, which can contaminate the MEA. Fortunately, the MEA restored more than 98% of its original performance after a simple treatment with 1 mol/L H$_2$SO$_4$ solution. This indicates the short period performance decline of the MEA is mainly caused by a recoverable contamination.

1. Introduction

Hydrogen is widely used in different industrial sectors, including chemical, metallurgical, electronic, power, aeronautic and astronautic industry. Moreover, hydrogen energy, with hydrogen being the cleanest energy carrier, is considered to be an ideal alternative to fossil energy in the future [1–5]. Hydrogen is produced in different ways, which can be classified as renewable or non-renewable hydrogen production [6,7]. Those depending on fossil fuels are non-renewable, whereas others consuming only water, biomass and solar energy are renewable.

Water electrolysis is the simplest and the most mature method of renewable hydrogen production [8]. The hydrogen produced presently by this method, however, is approximately 4% of the total H$_2$ production in the world [9]. This is mainly because water electrolysis requires high electricity consumption so that it is not yet able to compete with other fossil fuel dependent methods. However, water electrolysis might become a competitive hydrogen production method in the future [10], with the decline of global fossil fuel reserves, the ever growing availability of electricity from other renewable energy resources and the technology improvement of water electrolysis itself.

Solid polymer electrolyte (SPE) water electrolysis technology, first developed by General Electric in the 1960s for spacecraft applications [11], demonstrated significant advantages [12–14] over conventional alkaline electrolyte water electrolysis. The advantages include much less corrosive electrolyte, much higher volume specific hydrogen production capacity, higher product purity and higher efficiency. Therefore, SPE water electrolysis is considered to be a very promising technique of hydrogen energy.

The research on SPE water electrolysis is very active in recent years. Most of such research focused on novel cathode or anode catalyst systems [14–18]. In contrast to that, the research publications on membrane electrode assemblies (MEAs) are not many, although a great number of researches on the very similar MEAs for polymer electrolyte membrane fuel cells were reported [19–22].

While the stability and durability studies of the MEAs in water electrolysis are of crucial importance from the viewpoint of practical application, the number of reports on this subject is very limited. Andolfatto et al. [23] tested the stability of SPE water electrolysis at constant temperature and current density for over 5000 h. The cell voltage increase of the MEA using IrO_2/Ti as electrocatalyst was found 100–300 mV lower than that of the MEA with Pt electrocatalyst, indicating IrO_2 loaded on Ti support is more stable than Pt. Up to 20,000 h testing of an MEA having a Pt/Nafion/Pt sandwich structure was conducted by the same group [24]. Corrosion of the steel pipes of the electrolyzer and gaseous accumulation between the electrodes and their current collectors were found to cause major Ohmic losses or increase of the cell voltage.

Millet et al. [25] investigated the change of Pt and Pt–Ir anodes on their respective MEAs after 2500 h of water electrolysis at the current density of 1 A/cm². More numerous and wider cracks were observed from SEM micrographs as compared with the initial anodes. While the MEA with Pt–Ir anode showed decline of performance, no such change was found with the MAE having Pt anode.

Scherer et al. [26] compared MEAs fabricated with three different SPEs, namely Nafion117, CEC and RAI4010. The durability test at 80 °C and 1 A/cm² showed that the single cell voltage rose only 30–90m V after 10,000 h in the case of Nafion117 and CEC membranes, whereas the RAI4010 membrane showed a voltage increase by 570 mV after 3000 h. The authors attributed the sharply increased cell voltage to the degradation of the RAI4010 membrane. Both CEC and RAI4010 are partially fluorinated, with the degree of fluorination being 35% and 50%, respectively. However, the RAI4010 membrane was prepared by grafting sulfonated styrene on FEP/TFE Teflon matrix, whereas the CEC was made by grafting trifluorostyrene onto poly (tetrafluoroethylene–ethylene) followed by sulfonation of the aromatic styrene ring. Therefore, the authors suggested that the stability of the membrane depends on the particular fluorinated sites within the polymer chains.

In this research, MEAs were fabricated with Nafion112 membrane as the SPE and Ir black and Pt black as anode and cathode respectively. The stability of the MEAs was investigated by not only monitoring the performance decline of water electrolysis with the operation time, but also tracing any changes in the electrocatalysts and feed water by using different characterization methods. Restoration of the MEAs' performance by using facile method was also attempted.

2. Experimental

2.1. MEA preparation

To prepare anodic catalyst ink for an MEA of 4 cm² effective electrode area, 15.2 mg Ir black (He Sen Company, China), 39.0 mg of 5 wt% Nafion solution (DuPont), 0.5 mL deionized water, 0.5 mL isopropanol and two drops (about 100 μL) of glycerol were added to a glass beaker. The mixture was ultrasonically agitated for 60 min to obtain a homogenous suspension, the anodic catalyst ink. The cathodic catalyst ink was prepared similarly, with the Ir black substituted by 9.2 mg Pt black (Johnson Matthey) and the amount of 5 wt% Nafion solution changed to 20.2 mg.

The as-prepared anodic catalyst ink was spread on a sheet of silicon rubber and dried at 120 °C in an oven. This process was repeated a few times until all the ink in the beaker was used up. The cathodic catalyst ink was also transferred to a sheet of silicon rubber and dried in the same way.

The MEAs were prepared by a decal method, which is similar to that described by Wilson and Gottesfeld [27] A Nafion112 membrane was positioned between the two catalyst-loaded sheets of silicon rubber, with each's catalyst side facing the membrane. The sandwich was then clamped between two stainless steel plates and hot pressed at 130 °C and 8 MPa for 90 s, transferring the two catalyst layers from the rubber sheets to the two sides of the membrane. A three layered MEA was obtained after the sandwich was removed from the hot-presser, cooled at room temperature and peeled off the two rubber sheets.

The MEA was boiled in 1 mol/L H_2SO_4 solution for 30 min to protonate the Nafion SPE, then rinsed in boiling deionized water repeatedly to remove residual acid, and finally kept in deionized water prior to use.

The platinum loading and iridium loading on the two sides of the membrane were about 2.3 mg/cm² and 3.8 mg/cm², respectively.

2.2. Water electrolysis

A self-made single cell water electrolysis test stand was used to study the performance of the MEA (Fig. 1). The electrolytic cell 1 consists of the MEA, a piece of carbon paper (Toray) as cathode current collector, a 40 mesh titanium net as anode current collector and two titanium end plates with parallel flow channels. The power source 2 provides a direct electric current across the electrolytic cell, producing H_2 at the cathode and O_2 at the anode. Deionized water is fed by the pump 6 from the water tank 7 to the flow channels of the cathode side of the cell and flows back to the water tank. The flow rate of water entering the cell is monitored and regulated by the flowmeter 5 linked between the cell and the pump. The feed water is heated by the coil heater 8 in the tank and the water temperature in the cell is regulated via a control loop composed of the thermocouple 12, the temperature regulator 11, the electric relay 9 and power voltage regulator 10.
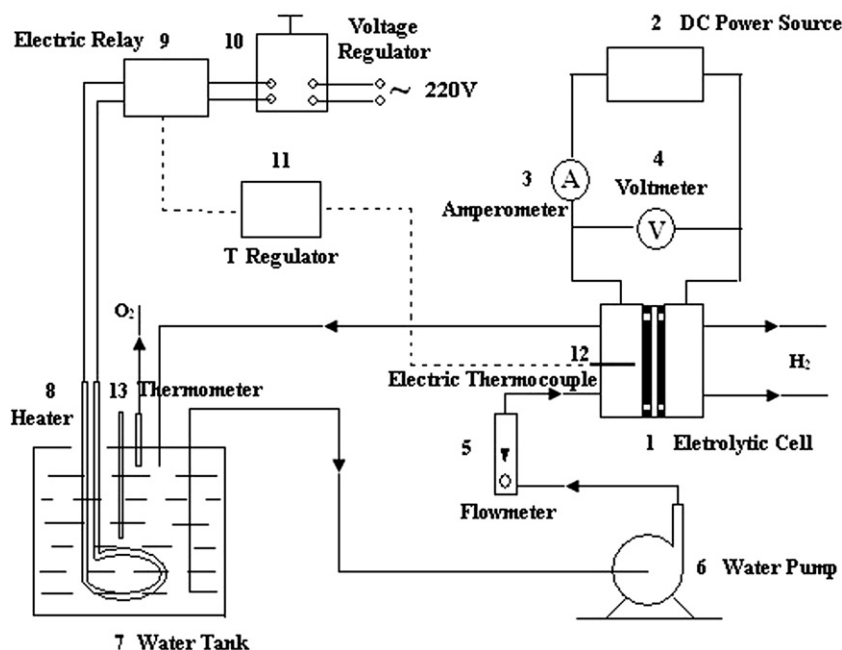
Fig. 1 – A schematic of the single cell test stand of water electrolysis.

The temperature of feed water in the electrolysis cell was set to 60 °C during the test and a fluctuation between 60 ± 1 °C was noticed. The water tank was refilled from time to time to ensure no noticeable change of the water level.

Two identical MEAs were tested under constant cell voltage 1.8 V, one for 208 h and the other 2 h. The 208 h tested MEA and the 2 h tested MEA will be hereafter designated as MEA-208 and MEA-2, respectively.

The V–I polarization curves of the MEAs were recorded by increasing stepwise the cell voltage from 1.2 V to 2.0 V, with an interval of about 1 min in each step to allow the cell current approaching steady state.

2.3. Characterizations and analysis

PHI 1600 X-ray photoelectron spectroscope (Perkin Elmer) and *X'pert PRO* X-ray diffractometer (PANalytical) were employed to characterize the chemical state and the structures of the catalysts. The catalyst specimens of the MEAs were cut from the MEAs' surfaces after their stability test (MEA-2) or restoration test (MEA-208).

Vista MPX inductively coupled plasma optical emission spectrometer (Varian, Inc.), *DX-600* ion chromatographer (Dionex), *DDS-307* conductivity meter (Shanghai Precision & Scientific Instrument) and $V_{CPH}TOC$ total organic carbon analyzer (Shimadzu) were employed for the analysis of trace elements, anions, ionic conductivity and total organic carbon in the feed water from the water tank.

3. Results and discussion

In the stability test, water electrolysis was run in a constant cell voltage mode. Consequently, a general trend of cell current decline, thus slowdown of hydrogen evolution, was observed

during the whole period of testing, as shown in Fig. 2. It is noted that the current density falls quickly from 680 mA/cm² to about 545 mA/cm² and then bounces up to 590 mA/cm², in the first 13 h or so. After that, the cell voltage continues to decrease wavily but almost linearly when viewed from the whole time scale, with a slope of 0.87 mA/cm² per hour.

In order to understand the observed declining of cell performance, both anodic and cathodic catalysts on the MEA-208 were characterized via XPS and XRD and were compared with the catalysts on the MEA-2.

There is no chemical change of the Pt catalyst along with the 208 h water electrolysis. This is revealed from a comparison of the XPS spectra of the Pt catalyst from pristine Pt black, MEA-2 cathode and MEA-208 cathode (Fig. 3). The Pt $4f_{7/2}$ peak
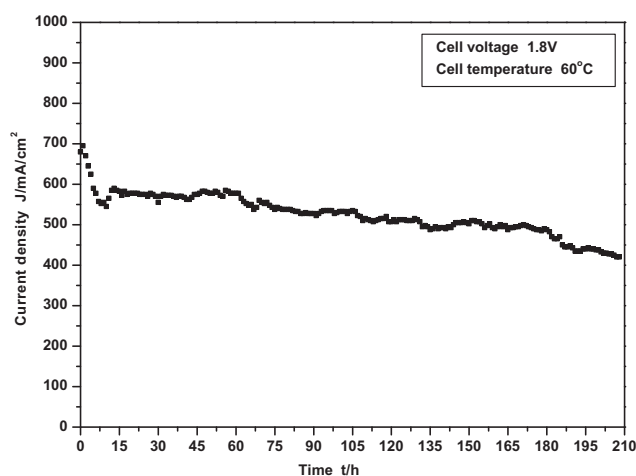

Fig. 2 – Cell current density varying with running time of water electrolysis in the stability test of the MEA at constant voltage mode.
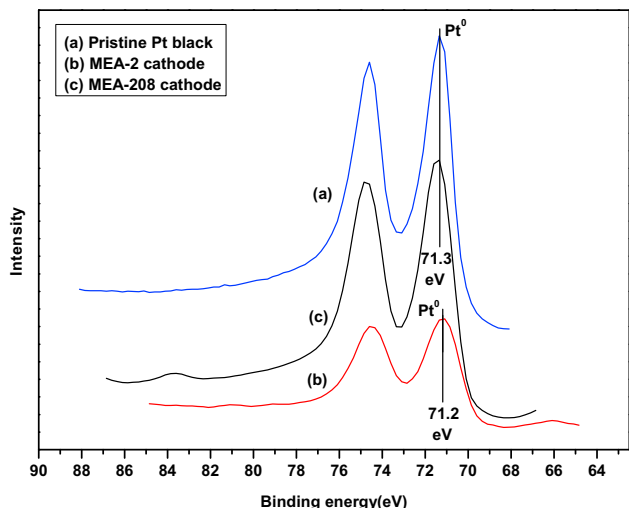
Fig. 3 – X-ray photoelectron spectra of Pt $4f_{5/2,\ 7/2}$ from (a) pristine Pt black, (b) MEA-2 cathode and (c) MEA-208 cathode.

Fig. 5 – X-ray diffraction patterns of (a) MEA-208 anode and (b) pristine Ir black.

of pristine Pt black appears at 71.3 eV of binding energy in its spectrum (Fig. 3(a)), which is expected for Pt in its metallic state [28]. Moreover, the Pt $4f_{7/2}$ peak binding energy in the Pt spectra of both MEA-2 and MEA-208 cathodes (Fig. 3(b) and (c)) is almost the same as that of pristine Pt black, indicating identical oxidation state of Pt in the three specimens.

However, an increase in the crystallite size of the Pt catalyst after 208 h of water electrolysis was detected through XRD measurement (see Fig. 4). As compared with the pristine Pt black, the Pt from MEA-208 cathode has a smaller half-peak width or FWHM [29] on its XRD pattern, despite of very identical characteristic diffraction angles of the Pt (111), Pt (200) and Pt (220) crystal planes. Calculation according to Scherrer Equation [29] shows that the crystallite size grew from the initial 9.1 nm to 9.8 nm after 208 h. If the particle size and XRD crystallite size of the Pt catalyst are assumed equal [29], the increase of crystallite size can translate to a decrease of catalyst area by about 7%.
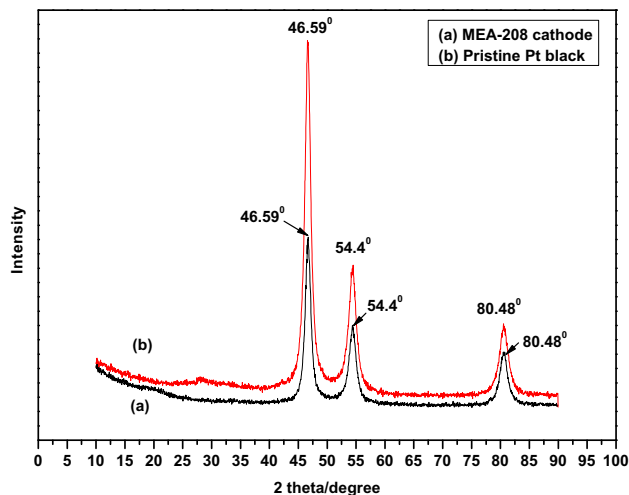
In contrast, the XRD crystallite size of Ir catalyst appears to remain unchanged, according to the XRD patterns shown in Fig. 5. The FWHM measured from the XRD pattern of Ir from MEA-208 anode (Fig. 5(a)) is very identical to that from pristine Ir black (Fig. 5(b)), indicating the original crystallite size of 3.5 nm has not been altered. However, the peaks at 46.78° and 83.0°, which are characteristic of Ir (111) and Ir (220) crystal planes [30], are noticed to have broadened tops (Fig. 5(a)), implying certain change happened related to the anodized Ir catalyst from MEA-208. An additional peak can be also noticed at $2\theta = 20°$ (Fig. 5(a)), which should be assigned to the Nafion polymer presented in MEA-208 anode. A smaller peak at the same diffraction angle exists in the XRD pattern of MEA-208 cathode (Fig. 4(a)), which is justified by the fact that there is less Nafion polymer in the Pt catalyst layer than in Ir catalyst layer.

An evidence of change in the anodized Ir catalyst was found from XPS measurement. The XPS spectra of Ir $4f_{5/2,\ 7/2}$
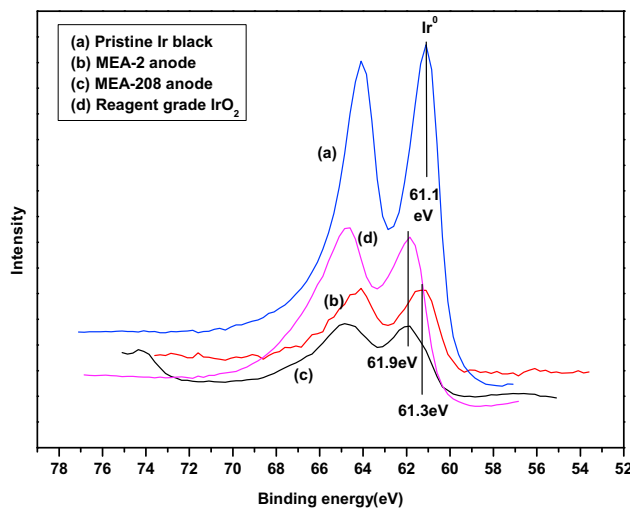

Fig. 4 – X-ray diffraction patterns of (a) MEA-208 cathode and (b) pristine Pt black.

Fig. 6 – X-ray photoelectron spectra of Ir $4f_{5/2,\ 7/2}$ from (a) pristine Ir black, (b) MEA-2 anode, (c) MEA-208 anode and (d) reagent grade IrO_2.
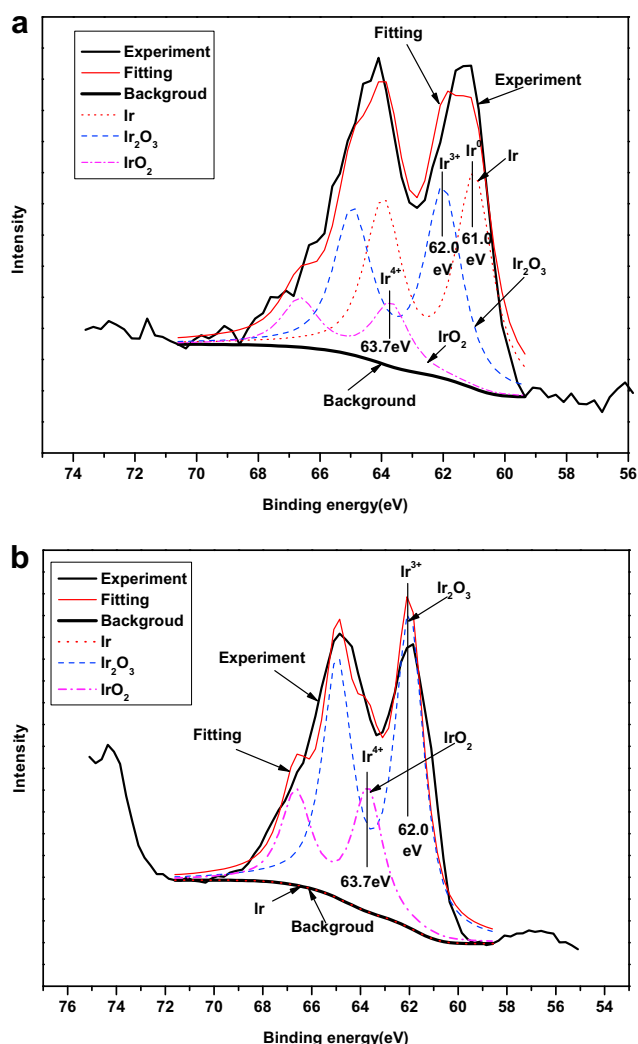
Fig. 7 – High resolution XPS spectra and fitting of Ir 4f$_{5/2, 7/2}$ from (a) MEA-2 anode and (b) MEA-208 anode.

Table 1 – Relative content of Ir species on the surface of anodic Ir catalyst by XPS data fitting.

%	Ir^0	Ir^{3+}	Ir^{4+}
MEA-2	45.7	40.7	13.6
MEA-208	0.0	71.5	28.5

detecting depth of 2–5 nm. Nevertheless, the oxidation of the Ir catalyst should only occur at a very thin surface layer, otherwise a more considerable change in its XRD pattern, other than the one shown in Fig. 5(a), would have resulted.

More details about the iridium oxide thin layers can be obtained through further analyzing the XPS data from MEA-2 and MEA-208 anodes (Fig. 6(b) and (c)). Based on the assignment of the specific Ir 4f$_{7/2}$ peak binding energy 61.0 eV, 62.0 eV, and 63.7 eV to Ir^0, Ir^{3+} and Ir^{4+} oxidation states [28], the overlapped peaks of the raw spectra were separated and fitted via the software XPSPEAK4.1, which enables relative atomic contents of the respective Ir species to be calculated (Fig. 7). The result reveals that more than 50% of Ir atoms on the surface of the catalyst were oxidized in 2 h. All Ir atoms on the surface of the catalyst were oxidized and more were oxidized to higher oxidation state after 208 h of water electrolysis. The relative contents of different Ir species on the surface of the Ir catalyst from the two MEAs are summarized in Table 1.

The surface oxidation of Ir catalyst can have quite different effects on its performance in water electrolysis. Iridium oxide conducts electricity much poorly than does metallic iridium, so the Ir particle with oxidized surface will have higher electrical resistance. Moreover, the contact resistance between such particles will also increase [33]. Therefore, the whole anode layer on the MEA can present higher Ohmic resistance, and thus lower current density at a given cell voltage, because of the surface oxidation of Ir catalyst.

However, iridium oxide is known to be a better catalyst than metallic iridium for oxygen evolution and shows lower electrochemical overpotential [34,35]. In this case, an increase in the current density at the same cell voltage should be expected with the oxidation of Ir catalyst.

The above mentioned contrary effects may, to certain extent, be attributed to the sharp fall and then up bounce of electrolytic current in the initial 13 h of MEA stability test (Fig. 2). Especially, the surface oxidation of the anodic Ir

from MEA-2 and MEA-208 anodes are shown in Fig. 6(b) and (c). For comparison, the corresponding spectra of pristine Ir black and a reagent grade IrO$_2$ are also included in the figure. Both the Ir 4f$_{7/2}$ peak binding energy at 61.1 eV and the 2.96 eV difference between the Ir 4f$_{7/2}$ and Ir 4f$_{5/2}$ peaks are in good agreement with previous measurements [28,31] and indicate that the detected Ir in the specimen of the pristine Ir black is in metallic state (Fig. 6(a)). On the other hand, it is natural to see the peak of Ir 4f$_{7/2}$ shifting to a higher binding energy of 61.9 eV in the spectrum of IrO$_2$ (Fig. 6(d)), for the Ir in iridium oxide should be in positive oxidation state.

The Ir 4f$_{7/2}$ peaks of MEA-2 and MEA-208 anodes (Fig. 6(b) and (c)) shift in between that of pristine Ir black and IrO$_2$. Moreover, the peak of MEA-2 anode moves not very far from that of pristine Ir black, while the two peaks of MEA-208 anode and reagent grade IrO$_2$ coincide with each other. This shows clearly the oxidation with time of the anodic Ir catalyst in the process of water electrolysis, which is also in agreement with the previous research [32].

It should be noticed the messages from XPS spectra are merely that of the surface of the specimens, owing to the set

Table 2 – Ionic species and TOC in the feed water at the start and finish of the 208 h test.

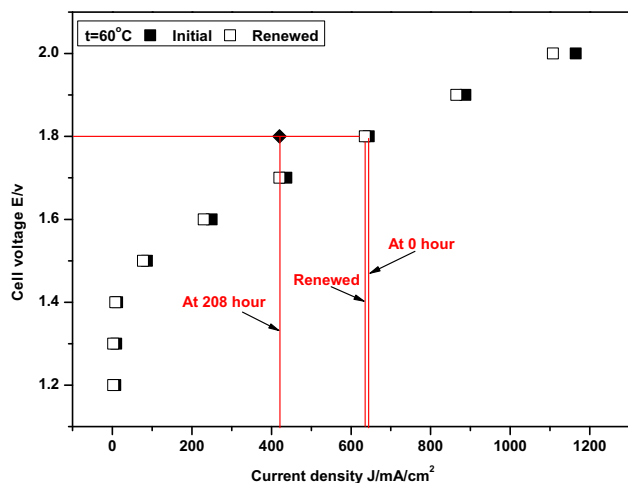| mg/L	At test start	At test finish
Cations		
Si	0.0000	0.4495
Na	0.0007	0.0025
Ca	0.0014	0.0081
Cr	0.0008	0.0007
Ni	0.0003	0.0000
Fe	0.0015	0.0012
Anions		
SO$_4^=$	0.0000	1.1472
NO$_3^-$	0.0000	0.9061
Total organic carbon	4.5630	0.5048

Fig. 8 – V–I polarization curves of the initial and renewed MEA-208.

catalyst should explain the up bouncing of the current, for the time of the two occurrences seems to match. In addition, the Ir surface oxidation could be the only factor that causes the electrolytic current to increase in the set circumstance, in contrast to the many factors that cause the current to decease.

Some of the factors that cause the current to decease were revealed through analyzing the feed water in the water tank. It was found that the ionic conductivity of the feed water has changed from the initial 1.46 μS/cm to 26.7 μS/cm at the end of the 208 h test. This tells roughly that the concentration of ionic species had increased by 18 times. More detailed information on the impurities was obtained via ICP-OES, ionic chromatography and TOC measurement and is summarized in Table 2. The table shows that there was a considerable accumulation of silicic, sulfate and nitrate components in the feed water with the process of water electrolysis. The cations of Na and Ca were also obviously increased, whereas the total organic carbon (TOC) decreased.

The impurities found should originate in part from the deionized water supplied for the experiment, which are not only concentrated with the water being electrolyzed, but also added from time to time with refilling the water tank. Other sources of impurity may be the water tank, the piping and other components of the test stand, which can be dissolved in trace amount by water. The silicic species detected, for instance, is speculated to come from the water tank made of nano-SiO_2 filled polypropylene, which seemed to be the only possible Si source.

Some impurities discovered may not be in its original form but have been chemically converted. Presumably, the microbes in the feed water, detected as TOC, were electrolyzed at the anode. Their sulfur and nitrogen containing organics can also be oxidized to sulfate and nitrate and carbon oxidized to CO_2 [36], which then escape from water. This would explain the large decrease of TOC and the appearance of $SO_4^=$ and NO_3^- in the feed water when the test finished.

The performance of MEA in water electrolysis can be affected by the impurities in a number of ways. Metal cations from feed water can contaminate MEA by exchanging with a portion of protons in the Nafion polymer electrolyte of the MEA. The contaminants in the polymer electrolyte will result

in higher resistance, or Ohmic overpotential, to the ionic conduction in the MEA, since a metal cation moves much slower than a proton does.

Driven by the cell voltage, the exchanged metal cations will travel across the Nafion membrane to the cathode side. Underpotential deposition of some of these metal cations, e.g. Ni^{2+}, could occur at the cathode [13,37]. The deposit of metal monolayer will cover the surface of the cathodic catalyst, thus hindering effective hydrogen evolution and causing increased electrochemical overpotential. Some other metal cations, e.g. Ca^{2+}, have very negative Nernst potential and cannot be reduced at the cathode. But they could precipitate as hydroxides [38] at the interface between the membrane and the cathode and block the active sites of the Pt catalyst. The hydroxide precipitates, having very poor electrical conductivity, will also increase Ohmic overpotential.

While the performance of MEA can be deteriorated by the contaminants in many ways, it should recover if they are removed. Therefore, a simple treatment of the MEA-208 was tried after the 208 h stability test. The MEA-208 was boiled in 1 mol/L sulfuric acid solution for 1 h followed by rinsing copiously with deionized water. The renewed MEA-208 turned out to perform nearly as good as the original, in term of V–I polarization curve (Fig. 8). The cell current at 1.8 V recovered from the lowest 420 mA/cm^2 to 635 mA/cm^2, a 98% restoration relative to the initial 645 mA/cm^2 of the MEA-208.

The dramatic effect of acid washing reveals that the contamination of the MEA is the main cause of its performance deterioration in the short period of 208 h. To maintain good performance, therefore, it is crucial to use high quality feed water. Equally important is to choose carefully the component materials, e.g. that for water tank and piping, of the water electrolysis system. Fortunately, the contaminants can be removed and performance restored to a large extent via the facile method of acid washing, which could be especially significant to practical large scale water electrolysis systems.

4.   Conclusions

Water electrolysis was conducted for 208 h with an MEA of Ir/Nafion/Pt structure to test its performance stability. Under a constant cell voltage mode, the cell current was found to decline almost linearly after a sharp fall at the beginning.

It is evidenced that the contamination of the MEA is the main cause of its performance deterioration in the short period of 208 h. Surface oxidation of the anodic Ir catalyst took place quickly and the crystallite size of the cathodic Pt was increased with the electrolytic process.

It was shown that the performance of the 208 h tested MEA can be largely restored via simply dilute acid washing. This could be especially significant to the long term efficient operation of industrial water electrolysis systems.

Acknowledgement

REFERENCES

[1] Viswanath RP. A patent for generation of electrolytic hydrogen by a cost effective and cheaper route. Int J Hydrogen Energy 2004;29:1191–4.

[2] Daniel M, Alessandro DE. Economical electrolyser solution. Int J Hydrogen Energy 2008;33:3041–4.

[3] Ahmad GE, Shenawy ETE. Optimized photovoltaic system for hydrogen production. Renew Energy 2006;31:1043–54.

[4] Meng N, Michael KHL, Dennis YCL. Energy and exergy analysis of hydrogen production by a proton exchange membrane (PEM) electrolyzer plant. Energy Convers Manage 2008;49:2748–56.

[5] Sawada S, Yamaki T, Maeno T, Asano M, Suzuki A, Terai T, et al. Solid polymer electrolyte water electrolysis systems for hydrogen production based on our newly developed membranes, part I: analysis of voltage–current characteristics. Prog Nucl Energy 2008;50:443–8.

[6] Song CS. Recent advances in catalysis for hydrogen production and fuel processing for fuel cells. Top Catal 2008;49:1–3.

[7] Abdel AHK, Shalabi MA. Non-petroleum routes to petrochemicals. Int J Hydrogen Energy 1992;17:359–67.

[8] Sang DH, Kee BP, Rana R, Singh KC. Developments of water electrolysis technology by solid polymer electrolyte. Indian J Chem Sect A 2002;41:245–53.

[9] http://www.hydrogenassociation.org/general/faqs. asp#howmuchproduced.

[10] Masson JP, Molina R, Roth E, Gaussens G, Lemaire F. Obtention and evaluation of polyethylene-based solid polymer electrolyte membrane for hydrogen production. Int J Hydrogen Energy 1982;7:167–71.

[11] Grigoriev SA, Porembsky VI, Fateev VN. Pure hydrogen production by PEM electrolysis for hydrogen energy. Int J Hydrogen Energy 2006;31:171–5.

[12] Nuttall LJ, Russell JH. Solid polymer electrolyte water electrolysis development status. Int J Hydrogen Energy 1980;5:75–84.

[13] Millet P, Pineri M, Rurand R. New solid polymer electrolyte composites for water electrolysis. J Appl Electrochem 1989;19:162–6.

[14] Marco B, Daniel G. Activation of ruthenium oxide, iridium oxide, and mixed Ru_xIr_{1-x} oxide electrodes during cathodic polarization and hydrogen evolution. J Electrochem Soc 1997; 144:573–81.

[15] Rasten E, Hagen G, Tunold R. Electrocatalysis in water electrolysis with solid polymer electrolyte. Electrochim Acta 2003;48:3945–52.

[16] Marshall A, Borresen B, Hagen G, Tsypkin M, Tunold R. Preparation and characterization of nanocrystalline $Ir_xSn_{1-x}O_2$ electrocatalytic powders. Mater Chem Phys 2005;94:226–32.

[17] Ma HC, Liu CP, Liao JH, Su Yi, Xue XZ, Wei X. Study of ruthenium oxide catalyst for electrocatalytic performance in oxygen evolution. J Mol Catal A Chem 2006;247:7–13.

[18] Tavares AC, Trasatti S. Ni + RuO_2 co-deposited electrodes for hydrogen evolution. Electrochim Acta 2000;45:4195–202.

[19] Wan CH, Lin MT, Zhuang QH, Lin CH. Preparation and performance of novel MEA with multi catalyst layer structure for PEFC by magnetron sputter deposition technique. Surf Coat Technol 2006;201:214–22.

[20] Reshetenko TV, Kim HT, Krewer U, Kweon HJ. The effect of the anode loading and method of MEA fabrication on DMFC performance. Fuel Cells 2007;7:238–45.

[21] Wee JH, Lee KY, Kim SH. Fabrication methods for low-Pt-loading electrocatalysts in proton exchange membrane fuel cell systems. J Power Sources 2007;165:667–77.

[22] Kim HS, Subramanian NP, Popov BN. Preparation of PEM fuel cell electrodes using pulse electrodeposition. J Power Sources 2004;138:14–24.

[23] Andolfatto F, Durand R, Michas A, Millet P, Stevens P. Solid polymer electrolyte water electrolysis: electro catalysis and long-term stability. Int J Hydrogen Energy 1994;19:421–7.

[24] Millet P, Andolfatto F, Durand R. Design and performance of a solid polymer electrolyte water electrolyzer. Int J Hydrogen Energy 1996;21:87–93.

[25] Millet P, Alleau T, Durand R. Characterization of membrane-electrode assemblies for solid polymer electrolyte water electrolysis. J Appl Electrochem 1993;23:322–31.

[26] Scherer GG, Takashi M, Kazuo T. Membrel-water electrolysis cells with a fluorinated cation exchange membrane. J Electrochem Soc 1988;135:3071–3.

[27] Wilson MS, Gottesfeld S. Thin-film catalyst layers for polymer electrolyte fuel cell electrodes. J Appl Electrochem 1992;22:1–7.

[28] Hara M, Asami K, Hashimoto K, Masumoto T. An X-ray photoelectron spectroscopic study of electrocatalytic activity of platinum group metals for chlorine evolution. Electrochim Acta 1983;28:1073–81.

[29] Suryanarayana C. Mechanical alloying and milling. New York: Marcel Dekker; 2004. p. 110–1.

[30] Hanawalt JD, Rinn HW, Frevel LK. Chemical analysis by X-ray diffraction: classification and use of X-ray diffraction patterns. Anal Chem 1938;10:457–512.

[31] Kötz R, Lewerenz HJ, Brüesch P, Stucki S. Oxygen evolution on Ru and Ir electrodes, XPS studies. J Electroanal Chem 1983; 150:209–16.

[32] Otten JM, Visscher W. The anodic behaviour of iridium, II: the oxygen coverage. J Electroanal Chem 1974;55:13–21.

[33] Mamunya YP, Zois H, Apekis L, Lebedev EV. Influence of pressure on the electrical conductivity of metal powders used as fillers in polymer composites. Powder Technol 2004; 140:49–55.

[34] Lu PWT, Srinivasan S. Advances in water electrolysis technology with emphasis on use of the solid polymer electrolyte. J Appl Electrochem 1979;9:269–83.

[35] Trasatti S. Electrodes of conductive metallic oxides part A. New York: Elsevier Scientific; 1980. p. 152–3.

[36] Han WQ, Wang LJ, Sun XY, Li JS. Treatment of bactericide wastewater by combined process chemical coagulation, electrochemical oxidation and membrane bioreactor. J Hazard Mater 2008;151:306–15.

[37] Kötz ER, Stucki S. Ruthenium dioxide as a hydrogen-evolving cathode. J Appl Electrochem 1987;17:1190–7.

[38] Abdel AHK, Husseina IA. Parametric study for saline water electrolysis: part III—precipitate formation and recovery of magnesium salts. Int J Hydrogen Energy 1993;18:553–6.